

# Snow depth estimation in the Indian Himalaya using multi-channel passive microwave radiometer

K. K. Singh<sup>1,\*</sup>, A. Kumar<sup>2</sup>, A. V. Kulkarni<sup>3</sup>, P. Datt<sup>1</sup>, S. K. Dewali<sup>1</sup>, V. Kumar<sup>1</sup> and R. Chauhan<sup>1</sup>

<sup>1</sup>Snow and Avalanche Study Establishment, Chandigarh 160 036, India

<sup>2</sup>National Institute of Technology, Kurukshetra 136 119, India

<sup>3</sup>Divecha Centre for Climate Change, Indian Institute of Science, Bengaluru 560 012, India

Snow depth is an important parameter for avalanche forecast and hydrological studies. In the Himalaya, manual snow depth data collection is difficult due to remote and rugged terrain and the severe weather conditions. However, microwave-based sensors in various satellites have the capability to estimate snow depth in all weather conditions. In the present study, experiments were performed to establish an algorithm for snow depth estimation using ground-based passive microwave radiometer with 6.9, 18.7 and 37 GHz antenna frequencies at Dhundhi and Patseo, Himachal Pradesh, India. Different layers in the snowpack were identified and layer properties, i.e. thickness, density, moisture content, etc. were measured manually and using a snow fork. Brightness temperature ( $T_B$ ) of the entire snowpack and of the individual snow layers was measured using passive microwave radiometer. It was observed that  $T_B$  of the snow is affected by various snow properties such as depth, density, physical temperature and wetness. A decrease in  $T_B$  with increase in snow depth was observed for all types of snow.  $T_B$  of the snowpack was observed higher at Dhundhi in comparison to Patseo. Based on the measured radiometer data, snow depth algorithms were developed for the Greater Himalaya and Pir-Panjajal ranges. These algorithms were validated with ground measurements for snow depth at different observatory locations and a good agreement between the two was observed (absolute error: 7 to 39 cm; correlation: 0.95).

**Keywords:** Brightness temperature, microwave radiometer, snow depth algorithm, snowpack.

THE Indian Himalaya covers an area of ~5 lakh sq. km and its terrain is highly rugged with limited accessibility<sup>1</sup>. In winter, most of the area remains snow-covered and the variation in deposited snow in terms of its areal extent and snow depth is very high. The inaccessible terrain poses great difficulty for monitoring snow cover/snowpack manually. Researchers have used snow and metrological

data collected through manned observatories and automatic weather stations (AWS) for snow and avalanche-related studies in the Himalaya<sup>2,3</sup>. These observatories/AWS are difficult to install and maintain in the Himalaya due to harsh weather conditions and complex topography. Moreover, these observatories provide point-based information and represent the snow-metrological conditions of the nearby areas.

Satellite-based remote sensing techniques, viz. optical and microwave, are potential tools for estimation of various snowpack-related parameters on a large spatial scale. Moreover, these techniques provide a way for development of various algorithms after rigorous ground validation, which can be used for retrieval of various snow properties from the larger area. The optical data are useful to retrieve snow surface properties and are mostly used for snow cover monitoring<sup>4</sup>, albedo estimation<sup>5</sup>, etc. However, the persistent cloudy conditions in the Indian Himalaya during winter season severely hamper the use of optical data for snow cover-related studies on a continuous basis. Apart from surface properties, snow depth also plays an important role for various applications such as snow melt run-off, snow water equivalent estimation and snow accumulation – an input for avalanche prediction.

Because of high penetrating capability of microwave in snow, it is being successfully used for estimation of snow depth and related parameters in all weather conditions<sup>6</sup>. The large variation in microwave signal due to the presence of water makes microwave data suitable for snow study. Snow remains mostly transparent for EM radiations below 9 GHz; however, at higher frequencies the response of different snow parameters on the brightness temperature ( $T_B$ ) can be observed. New/dry and wet snow behave entirely different in microwave region. In wet snow two geometries are common, i.e. snow with a low free-water content (<7% by volume) and snow with a high free-water content (>7% by volume)<sup>7</sup>. Microwave emission emanating from a snowpack consists of emission from the snow volume and from the underlying ground<sup>8</sup>. The scattering of microwave radiations is more

\*For correspondence. (e-mail: kamal.kant@sase.drdo.in)

pronounced at the shorter wavelengths for dry snow having large particle size. Larger snow grains formed possibly due to ageing or melt–freeze cycles, increase scattering and reduces the  $T_B$  (ref. 9). In order to model the microwave emissions from the snowpack, Wiesmann and Mätzler<sup>10</sup> developed a microwave emission model of layered snowpack (MEMLS).

In the Indian Himalaya, snow depth and ice thickness measurements were also carried out using radio echo sounding techniques<sup>11,12</sup>. However, these techniques are site-specific and measurements cannot be generalized with the help of any algorithm. Most of the research regarding snow depth and snow water equivalent estimation was carried out at relatively homogeneous flat areas such as the Canadian high plains and the Russian steppes using an empirical relationship between snow depth, snow water equivalent and  $T_B$  at 19 and 37 GHz frequencies<sup>13,14</sup>. Work has also been reported to relate microwave emission and various other snow parameters, i.e. mean snow grain size and density, etc.<sup>9,15–17</sup>. The space-borne passive microwave radiometer data (SSM/I and AMSR-E) have been used to estimate snow depth at a few places in the Indian Himalaya<sup>6,18</sup>. In these studies estimated snow depth from satellite-derived  $T_B$  was observed in good correlation with the ground observed snow depth. Ground-based passive microwave radiometer can provide  $T_B$  measurements which may be used for development of an algorithm for snow depth estimation with higher accuracy, apart from ground validation of the satellite data.

In the present study ground-based passive microwave radiometer having antenna frequencies 6.9, 18.7 and 37 GHz was used to observe the variation of  $T_B$  with varying snow properties. Various snowpack properties of different layers such as thickness, density, type, temperature, etc. were measured manually/derived using snow fork. The emphasis of the study is to develop a simple and fast methodology for snow depth estimation using the data collected from ground-based passive microwave radiometer, which can be further applied for large areas. MEMLS was used to simulate the  $T_B$  values of the snowpack and were also compared with ground-based passive microwave radiometer data.

### Instruments and data used

Ground-based passive microwave radiometers at 6.93, 18.7 and 37 GHz frequencies were used in the study (Figure 1). Description of 6.93 and 18.7 GHz antennas is given in Singh *et al.*<sup>19</sup>. The 37 GHz radiometer is a Dicke radiometer similar to 6.93 and 18.7 GHz. The radiometers receive simultaneously both orthogonal polarizations – vertical (V) and horizontal (H) and are precise as they eliminate gain fluctuations. The radiometers were mounted on a mechanical arrangement. The mechanical mounting had the facility for setting the azimuth (0–360°) and

elevation (0–150°). The stand with 2 m adjustable height had the provision for mounting the radiometers in such a way that they can observe the zenith and surface of the ground. The facility of fixing the radiometers at any desired view angle was also available in the mounting arrangement. In order to provide the necessary accuracy and measurement stability, radiometers were placed in a thermostat and equipped with calibration systems.

The temperature inside the radiometer box was stabilized at the level of about 50°C to reduce gain variations and to provide stable noise temperature of the receiver. The output analogue signals corresponding to both V and H polarizations as well as signals from temperature sensors installed on the antenna and receiver were sent to the data acquisition system (DAS).

A snow fork from Toikka, Finland (Figure 2) was used for the measurement of snowpack parameters. This



**Figure 1.** Passive microwave radiometer at Dhundhi (Himachal Pradesh).



**Figure 2.** Snowpack dielectric profiling using snow fork.

instrument uses a steel fork as a microwave resonator and measures the electrical parameters like resonant frequency, attenuation and 3 dB bandwidth for estimating both real and complex dielectric parts. Snowpack liquid water content and snow densities were derived using empirical relations given by Denoth<sup>20</sup> and a user/technical manual<sup>21</sup>. For collection of snowpack data, a vertical pit was dug carefully and measurements were taken by inserting the snow fork horizontally at 10 cm depth intervals on the shaded wall of pit to avoid direct radiation on the snow fork. The instrument was calibrated after each set of measurements and its fork was wiped to remove water after each reading.

In order to validate the developed snow depth algorithms, satellite data of Advanced Microwave Scanning Radiometer-Earth (AMSR-E) sensor were used and the snow depth values at different locations in NW Himalaya were estimated. AMSR-E is a six-frequency total power microwave radiometer system with dual polarization capability for all frequency bands. Details of the AMSR-E sensor are given in Table 1.

### Study area

Radiometer experiments were carried out at two field observatories situated in different mountain ranges of NW Himalaya, having different snow climatic conditions (Figure 3). In Pir-Panjal, radiometer data were collected at snow-metrological observatory location of the Snow and Avalanche Study Establishment (SASE) Dhundhi, Himachal Pradesh (HP) (lat. 32°21'19.5"N and long. 77°07'42"E). The altitude of the location is around 3050 m and it experiences heavy snowfall with snowpack having near isothermal conditions. The ambient temperature of this region remains higher in comparison to that of the Greater Himalayan region and because of this generally snow remains moist even in peak winter months. Mean seasonal air temperature in the Dhundhi sector has varied between -1.5°C and 2.8°C for the past 19 years and seasonal snowfall in this sector lies between 255 and 1186 cm with an average of 817 cm (ref. 22).

The second experimental site Patseo (HP, lat. 32°45'18"N and long. 77°15'43"E) lies in the Greater

Himalayan range, at an altitude of about 3800 m amsl. This area experiences high wind, relatively lesser snowfall and lower temperature in comparison to that of the Pir-Panjal range. Slopes are barren/rocky with scanty trees at the lower altitude level or valley bottom. The mean seasonal air temperature in this region during the past 22 years has varied between -5.9°C and -10.7°C and the seasonal snowfall lies between 134 and 410 cm with a 22 years average of 261 cm (ref. 22).

### Methodology

The methodology of the work presented is described in Figure 4. As the emission characteristics of snowpack depend on various parameters, it is important to measure them with high accuracy. In snowpack characterization, data of various snowpack parameters, i.e. snow layer thickness, layer density, layer type, layer temperature, etc. were collected manually. Apart from this, snow fork was used to collect some of the snowpack parameters, i.e. dielectric constant and volumetric water content in different snow layers.

Calibration of the radiometer was carried out with reference to highly absorbing black body and sky. Radiometer data corresponding to black body and sky were collected, and based on their respective temperature and voltage, linear equations were established, which were used for the measurement of  $T_B$ .

$T_B$  is equivalent to the intensity of the radiation emitted from the material and is expressed in Kelvin. The relationship between  $T_B$  and its physical temperature is expressed in eq. (1)

$$T_B = eT, \quad 0 < e < 1, \quad (1)$$

where  $e$  is the emissivity of the target.

The radiometer data of entire snowpack (Figure 5a) and of different layers were collected by removing snow layers one by one from the top (Figure 5b) and the corresponding  $T_B$  values were measured. The variation of  $T_B$  with different snowpack parameters was analysed and algorithms for snow depth estimation were formulated.

The validation of algorithms was done using the AMSR-E sensor data. The  $T_B$  values at different frequencies and polarizations were extracted for various locations of SASE in the Indian Himalaya by processing AMSR-E data in ENVI and ArcGIS software. Preprocessing and importing of the raw AMSR-E data were done using ENVI data import tools. A model in ArcGIS modeler was written to extract the  $T_B$  values from AMSR-E satellite data at different point locations. In this model feature location and attribute-based data extraction tools were used. These satellite estimated  $T_B$  values were further used to find the snow depth using the developed snow depth algorithm. The results were validated with the manually measured snow depth data.

**Table 1.** Specifications of AMSR-E sensor

Centre frequency (GHz)	Band width (MHz)	Sensitivity (K)	IFOV (km × km)
6.9	350	0.3	76 × 44
10.7	100	0.6	49 × 28
18.7	200	0.6	28 × 16
23.8	400	0.6	31 × 18
36.5	3000	0.6	14 × 8
89.0	1000	0.1	6 × 4

IFOV, Instantaneous field-of-view.

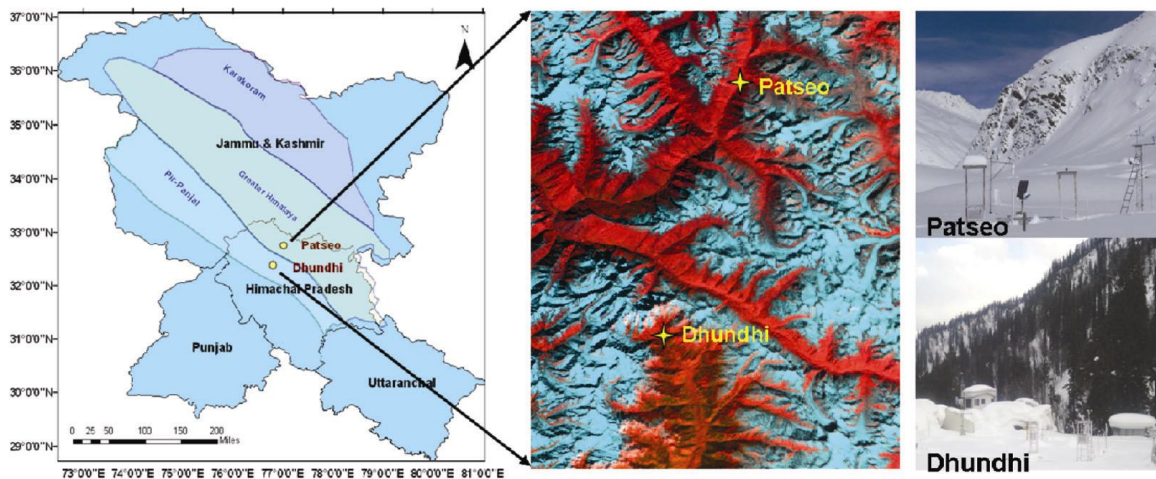


Figure 3. Study area for passive microwave radiometer experiments.

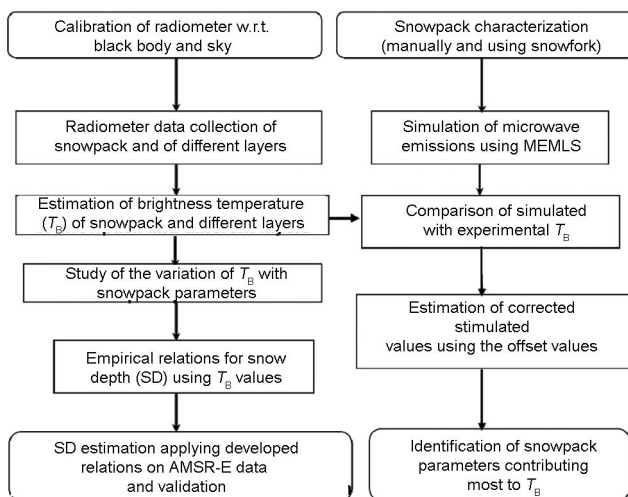


Figure 4. Flow chart of the methodology.

MEMLS was used to simulate emissions from the snowpack. This model uses correlation function approach and takes into account multiple scattering of radiation caused by stratification and snow grains, refraction and trapping of radiation, total internal reflection, and coherent and incoherent superposition of radiation by layer interfaces. The results of MEMLS were further compared with the ground-based passive microwave radiometer data.

## Results and discussion

### Field experiment at Dhundhi (Pir-Panjal range)

To study the response of  $T_B$  to different snow properties, an experiment was conducted at Dhundhi on 13 March 2009. The stratigraphy of the snowpack with snow parameters of each snow layer is given in Table 2.

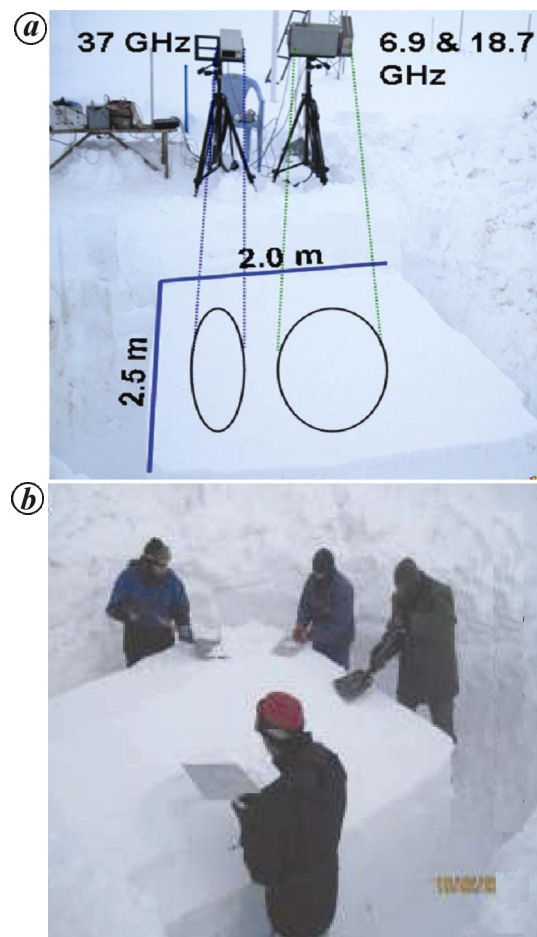


Figure 5. Field experiments for snow depth estimation. *a*, Data collection using radiometer; *b*, removal of snow layer.

The experiment was conducted in late winter and the thickness of the snowpack was observed to be only 58 cm; however, seven layers were identified in the snowpack. These layers were marked as L7 to L1 from the top. All

**Table 2.** Snowpack parameters (Dhundhi, Himachal Pradesh)

	Manually measured snowpack parameters				Snow fork-measured snowpack parameters				
	Layer thickness (cm) from top	Layer hardness	Layer wetness	Layer temperature (°C)	Grain type	Grain size (mm)	Layer volumetric water content	Layer density (g/cm <sup>3</sup> )	Layer dielectric constant
L7	58–51	Hard	Very wet	0	MF	4–5	8.5	0.41	2.90
L6	51–47	Hard	Wet	–1.0	MF	4–5	4.4	0.40	2.24
L5	47–40	Hard	Wet	–1.0	MF	4–5	6.0	0.31	2.35
L4	40–36	Hard	Wet	–1.0	MF	4–5	6.3	0.44	2.58
L3	36–25	Medium	Wet	–1.0	MF	4–5	5.9	0.45	2.55
L2	25–20	Hard	Wet	–1.0	MF	4–5	7.1	0.47	2.77
L1	20–0	Very hard	Very wet	0	MF	2–3	8.1	0.43	2.85

MF, Melt freeze grains.

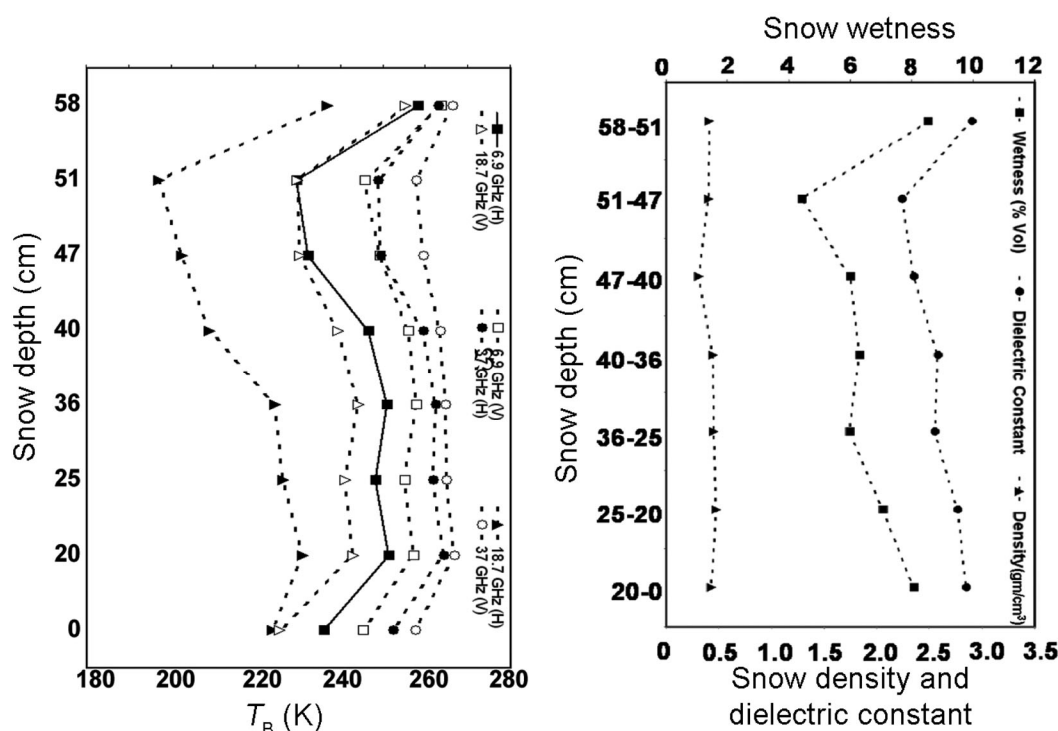


**Figure 6.** Variation of  $T_B$  with different snow properties.

the layers were of high density varying from 0.4 to 0.49 g/cm<sup>3</sup> and having high water content. The ambient temperature during the experiment was 10°C and snow surface temperature (SST) was 0°C. Because of high ambient temperature, the top surface of snow had very high moisture content in comparison to other snow layers in the snowpack. To analyse the variation of  $T_B$  with different snow layers properties, the layers were removed one by one from the top and the corresponding  $T_B$  values were measured using the radiometer.

From the graph in Figure 6, high values of  $T_B$  were observed corresponding to the entire snowpack (when the deposited snow was 58 cm) at all used microwave frequencies, i.e. 6.9, 18.7 and 37 GHz. These higher values of  $T_B$  may be due to the high ambient temperature which

has introduced high moisture in the snowpack, mainly in the top snow layer. Because of this high amount of moisture, water coats the snow grains and causes a significant increase in internal absorption of the microwave radiation. This absorption further decreases the volume scattering of the microwave radiations and as a result causes an increase in the snow emissivity and simultaneously the  $T_B$  values.

Once the highly wet top (L7) layer was removed, for all the frequencies a sharp decrease in  $T_B$  was observed. This decrease is due to lower wetness of the remaining snowpack. However, the polarization difference at 18.7 GHz was observed to be significantly increased and the gradient in decrease of  $T_B$  at 18.7 GHz was also high in comparison to 6.9 and 37 GHz with the removal of top

**Table 3.** Snowpack parameters (Patseo, Himachal Pradesh)

	Manually measured snowpack parameters					Snow fork-measured snowpack parameters			
	Layer thickness (cm) from top	Layer hardness	Layer wetness	Layer temperature (°C)	Grain type	Grain size (mm)	Layer volumetric water content	Layer density (g/cm <sup>3</sup> )	Layer dielectric constant
L7	181–179	Soft	Moist	–4.8	PP	4–5	0.4	0.07	1.17
L6	179–138	Soft	Moist	–7.6	PP	4–5	0.26	0.11	1.23
L5	138–118	Soft	Moist	–4.5	DF	4–5	0.55	0.16	1.34
L4	118–107	Medium	Moist	–4.3	DF	4–5	1.06	0.21	1.49
L3	107–57	Medium	Moist	–4.2	DF	4–5	0.91	0.30	1.64
L2	57–31	Soft	Moist	–2.8	FC	4–5	0.91	0.29	1.62
L1	31–0	Very soft	Moist	–1.7	DH	2–3	1.32	0.20	1.49

PP, Precipitation particle; DF, Decomposed fragmented; FC, Faceted and DH, Depth hoar.

layer. The water vapour absorption band near 22 GHz (H) frequency may be the possible reason for the above-mentioned observations and because of this 18.7 GHz was observed to be highly sensitive to the change in moisture content.

Further, the snow layers were removed one by one and an increase in  $T_B$  was observed till the removal of layer L2. With the removal of snow layers the snowpack thickness was reduced, which resulted in lesser number of ice particles which are responsible for scattering the microwave signals. Thus, because of this reduction in the number of scatters, increase in  $T_B$  was observed. The removal of the last layer above the ground ( $L_1$ ) resulted in some reduction in  $T_B$  values at all frequencies, which may be due to lower emissivity of the wet ground in comparison to that of wet snow. Results show good contrast in V and H polarization for the wet land at 6.9 and 37 GHz frequencies; however, very low contrast in both the polarizations was observed at 18.7 GHz frequency. From Figure 6, higher values of  $T_B$  were observed at 37 GHz frequency in comparison to 6.9 and 18.7 GHz. However, in the case of dry snow, generally the lower frequencies have higher  $T_B$  values because of low losses in the microwave range, while at higher frequencies the losses were high, as scattering becomes most prevalent at higher frequencies<sup>23</sup>. As the experiment was conducted in wet/very wet snow conditions, the higher values of  $T_B$  at 37 GHz frequency may be due to higher emissivity value at 37 GHz frequency for wet/very wet snow in comparison to the other frequencies, i.e. 6.9 or 18.7 GHz. Thus the higher values of  $T_B$  in 37 GHz frequency in comparison to 6.9 and 18.7 GHz can be used as an indicator to identify the wet snow zones.

#### *Field experiment at Patseo (Greater Himalaya range)*

An experiment was conducted at Patseo on 18 February 2011 (Greater Himalaya), to observe the variation of  $T_B$  with different snow parameters. Details of the snowpack are discussed in Table 3. As the experiment was carried out during peak winter, the snowpack depth was observed

to be 181 cm. A total of seven layers marked as L7 to L1 from the top of the snowpack were observed. All the layers were dry/moist with volumetric water content varying between 0.26 and 1.32. The average density of the snowpack varied between 0.07 and 0.30 g/cm<sup>3</sup>. The complete experiment took around 4 h and in this duration the ambient temperature varied between –7°C and –12°C; however the SST varied between –4°C and –11°C. Thus, because of negative ambient temperature and SST, very less amount of moisture content was observed in the snowpack.

Snowpack of dimension 2 m × 2.5 m × 1.81 m was isolated from the snow cover to study the response of varying snow properties with  $T_B$  at 18 and 37 GHz frequencies. Figure 7a shows the variation of  $T_B$  with change in snow depth, which is due to the removal of snow layers one by one from the top of the snowpack. From the figure higher  $T_B$  values were observed for the ground, which may be due to its high temperature. Decrease in  $T_B$  was observed with increase in snow depth up to 118 cm or L4 level. As with increase in snow depth, the ice particles responsible for scattering the microwave radiations also increased and this resulted in a decrease in  $T_B$  values with snow depth. However, from layer 5 onwards an increase in  $T_B$  values with snow depth was observed and this may be due to the lower values of snow density in snow layers L5–L7 as given in Table 3. Higher values of  $T_B$  were observed at 18.7 GHz (H) frequency in comparison to the 37 GHz (H), as the scattering high in 37 GHz in comparison to the 18 GHz frequency for dry/moist snow. The 37 GHz (V) frequency channel did not show the variation of  $T_B$  with varying snow properties; this may be due to some problem in the channel during the field experiment. Figure 7b shows the variation of snowpack parameters, i.e. snow density, snow wetness and dielectric constant with snowpack depth.

#### *Comparison of measured $T_B$ values of snowpack at Patseo and Dhundhi*

Comparison of  $T_B$  data of the snowpack collected using radiometer at Patseo and Dhundhi is shown in Figure 8. A total of seven layers were observed in the snowpack at both

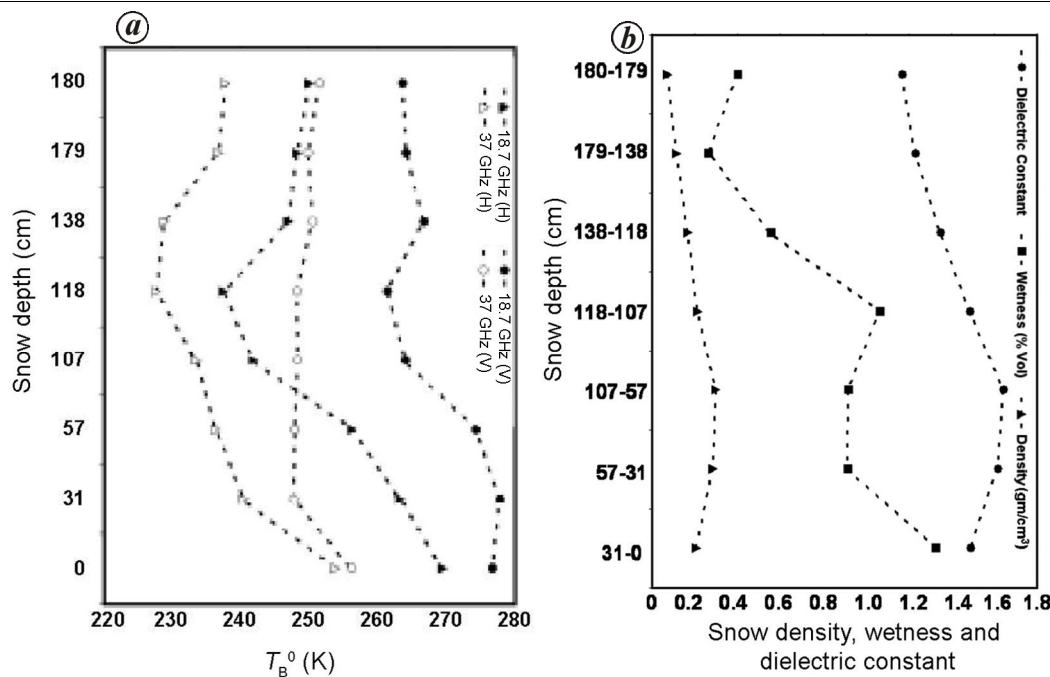


Figure 7. Variation of (a)  $T_B$  and (b) snow parameters with snow depth.

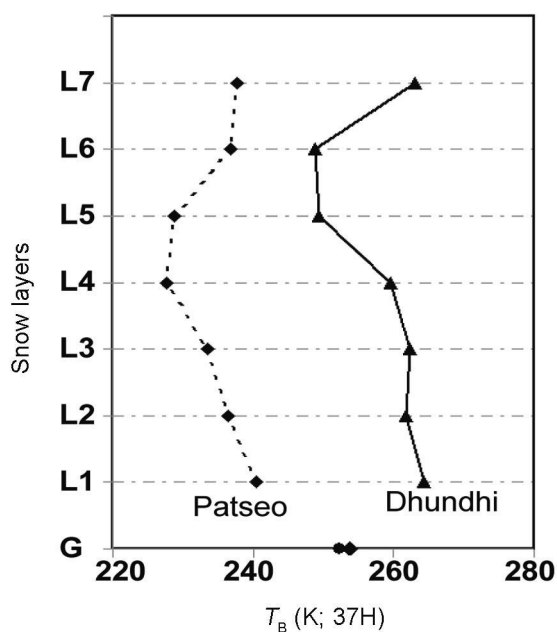


Figure 8. Comparison of  $T_B$  of snowpack at Dhundhi and Patseo. G, Ground surface; L1, Layer 1 immediately above the ground; L2, Next layer above L1, and L3–L7, Layers in the sequence above ground in the snowpack.

the locations; however, the snowpack depth was found different. From the graph higher  $T_B$  at 37 GHz frequency was observed for the snowpack at Dhundhi in comparison to that at Patseo. This may be due to the difference in moisture content, density and physical temperature of snow as given in Tables 1 and 2. A difference in  $T_B$  of

approximately 20 K has been observed between the snowpacks at both the places. A significant reduction in  $T_B$  values of the snowpack was observed after removal of the top two layers, both at Dhundhi and Patseo.

*Simulation of emissions from the snowpack using MEMLS*

To understand the influence of snowpack properties on the microwave emissions, simulation has been carried out using MEMLS model. This is a multiple-scattering model allowing many layers to simulate snow cover emission. The input file of snowpack parameters used in MEMLS consists of layer thickness, temperature, density, volumetric liquid–water content, correlation length ( $P_c$ ) and exponential correlation length ( $P_{ex}$ ). For the present study values of  $P_c$  and  $P_{ex}$  were directly taken from Mätzler<sup>24</sup>, where these values are given with respect to varying density, snow type and snow grain size.

The results of the simulation are presented in Figure 9 a and b, which shows the variation of  $T_B$  with change in frequency for vertical and horizontal polarization respectively. The simulation of the emission was carried out for the complete snowpack and after removing snow layers one by one from the top. From Figure 9 a and b, it can be observed that  $T_B$  decreases with frequency at both polarizations. Very low variation was observed between the simulations of the snowpack before and after removal of the top snow layer. Variation in  $T_B$  between intact snowpack and after removal of layers was observed to be high at higher frequencies. From these simulations,  $T_B$  was

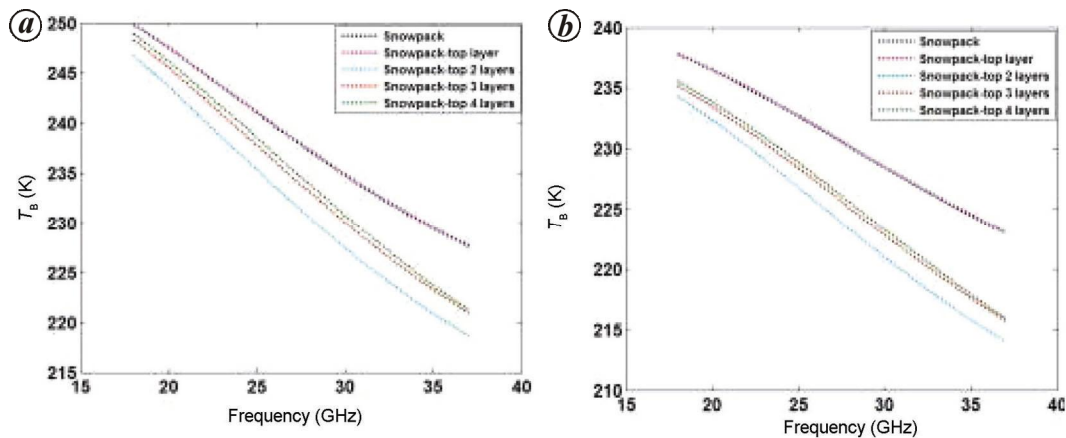


**Figure 9.** Variation of  $T_B$  with frequency for varying snowpack characteristics: *a*, V-Pol; *b*, H-Pol.

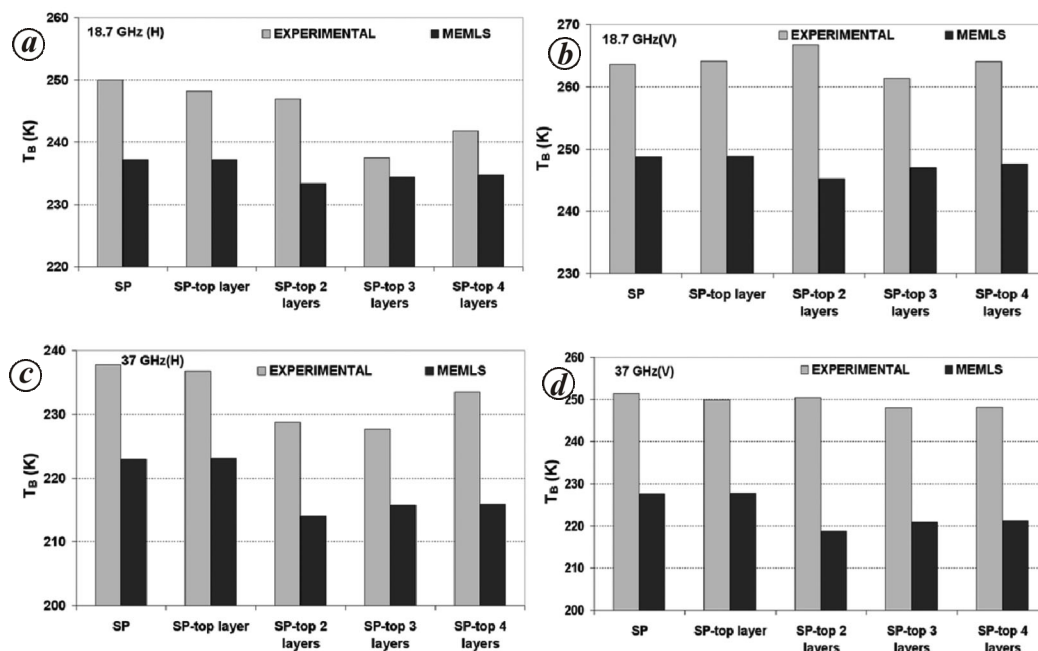


**Figure 10.** Comparison of experimental and MEMLS output  $T_B$  values: *a*, 18.7 H; *b*, 18.7 V; *c*, 37 H; *d*, 37 V.

estimated at 18.7 and 37 GHz frequencies and further compared with the experimental values.

Comparison of simulated and experimental results is shown in Figure 10.  $T_B$  of the snowpack depends mainly on the average grain size and temperature profile of the snowpack. From the graphs it can be observed that the simulated and experimental (observed)  $T_B$  values differ significantly. The simulated  $T_B$  values were underestimated for all the frequencies and polarizations. The possible reason of this may be the contribution of emissions from the ground in the experimental values, which are not considered in the simulation. In the simulation, the average temperature of the snowpack was estimated using the near ground temperature as  $-1.7^\circ\text{C}$ , as mentioned in Table 3. However, as the penetration of 18.7

and 37 GHz frequencies is more than 2 m in dry snow, thus the emissions are actually coming from deep inside the ground, where the temperatures are much higher. These soil emissions are an integral part of the radiometer collected data, hence the experimental  $T_B$  was observed to be higher in comparison to the MEMLS values.

The root mean square error (RMSE) values between the simulated and observed  $T_B$  were 9.6 K at 18.7H, 16.6 K at 18.7 V, 15.1 K at 37 H and 26.6 K at 37 V (Table 4).

The estimated mean absolute error values were further used as the correction values in simulation. These values at different frequencies and polarizations were added to the simulations to make them closer to the experimental (observed) values. Passive microwave radiometer data of dates 21 and 27 February 2011, collected at Patseo, were

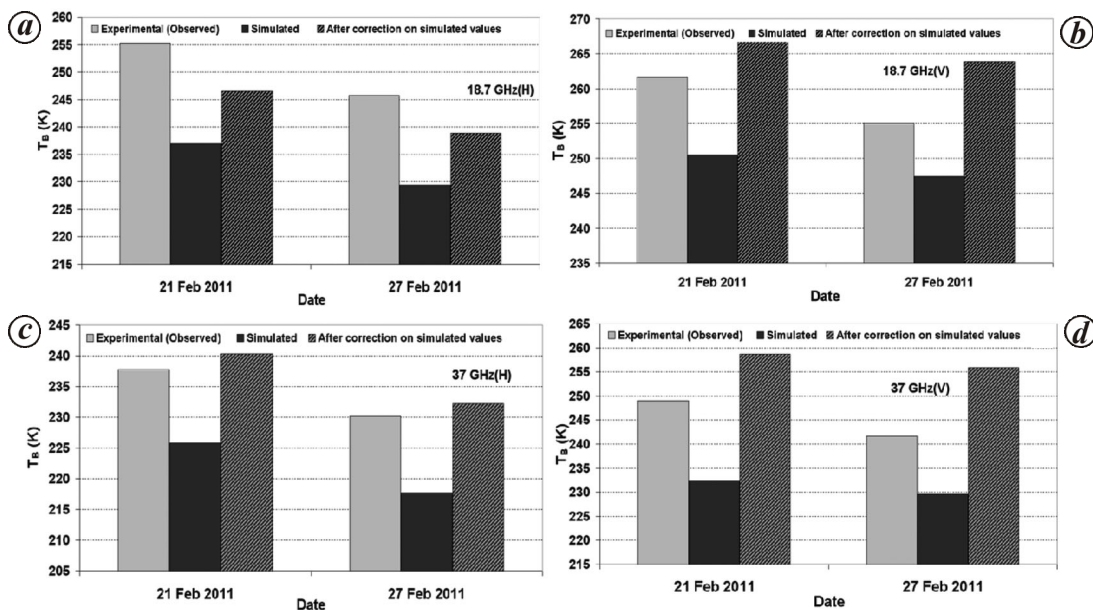


Figure 11. Comparison of experimental, simulated and corrected simulated  $T_B$  values: a, 18.7 H; b, 18.7 V; c, 37 H; d, 37 V.

Table 4. Error in simulations

Frequency (GHz)	Mean absolute error (K)	Root mean square error (K)
18.7 (H)	9.5	9.6
18.7 (V)	16.5	16.6
37 (H)	14.5	15.1
37 (V)	26.3	26.6

used to observe the change in simulation after applying the corrections in the simulated  $T_B$  data. Figure 11 shows the comparison between experimental, simulated and correction-applied simulated values. It was observed that after applying the corrections, the simulated values becomes closer to the experimental (observed)  $T_B$  values and the RMSE values between the correction-applied simulated and observed  $T_B$  were 8.7 K at 18.7 H, 7.3 K at 18.7 V, 4.6 K at 37 H and 12 K at 37 V.

The MEMLS output was further used to identify the prominent snowpack parameters affecting  $T_B$ . The data presented in Table 5 were used to relate the  $T_B$  variation with frequency with various other snowpack parameters, i.e. weighted average density, weighted average wetness, depth and weighted average snowpack temperature. The change in  $T_B$  with frequency for the snowpack before and after removal of snow layers one by one from the top was calculated by estimating the slope of the simulated  $T_B$  at horizontal and vertical polarization, as given in Figure 9. This estimated slope was further related with other snowpack parameters. The weighted average density of the snowpack was estimated to be 0.16 g/cm<sup>3</sup>, wetness 0.80 and temperature 268 K. A change in these parameters was observed with the removal of snow layers, as given in Table 5. The weighted average density of the snowpack

after removing the top five snow layers was 0.24 g/cm<sup>3</sup>, wetness 1.13 and temperature 270 K.

In order to avoid the redundancy of snow pack parameters in the regression analysis between  $T_B$  and density, temperature, depth and wetness of the snow pack, correlation coefficients of different parameters with each other were estimated (Table 6). After analysis, it was observed that snowpack depth had high correlation with snowpack wetness (0.98) and snowpack temperature (0.99), while snowpack temperature had high correlation with snowpack wetness (0.98) and depth (0.99). Thus among these three parameters, i.e. wetness, temperature and depth, snow wetness was chosen for this study to estimate how along with snow density it affects the snowpack  $T_B$ .

Linear regression analysis was applied on the data to develop a relationship between rate of change of  $T_B$  with density and wetness of the snow pack. The developed relation (eq. (2)) can be further used for estimation of rate of change of  $T_B$  within frequency range 18–38 GHz at vertical and horizontal polarization respectively.

$$\begin{aligned}
 S_V &= 1.12 - 11.01 \times \rho - 0.70 \times w, \\
 S_H &= 1.3 - 10.20 \times \rho - 0.59 \times w,
 \end{aligned}
 \tag{2}$$

where  $S_V$  and  $S_H$  are the slope of lines showing  $T_B$  variation with frequency at vertical and horizontal polarization respectively,  $\rho$  is the density and  $w$  is the snowpack wetness.

#### Snow depth estimation using passive microwave radiometer data

Data collected during field experiments at both Dhundhi and Patseo were further used to develop algorithms for snow depth estimation. For Patseo as the snow condition

**Table 5.** Snowpack and simulated data used in the study

	Slope of line (k/Hz; H-Pol)	Slope of line (k/Hz; V-Pol)	Weighted average snowpack density (g/cm <sup>3</sup> )	Weighted average snowpack wetness (vol. %)	Snowpack depth (cm)	Weighted average snowpack temperature (K)
Snowpack	-0.80	-1.20	0.16	0.80	180	268
Snowpack-top layer	-0.79	-1.19	0.16	0.80	179	268
Snowpack-top two layers	-1.10	-1.51	0.17	0.96	138	269
Snowpack-top three layers	-1.05	-1.48	0.17	1.03	118	269
Snowpack-top four layers	-1.06	-1.49	0.17	1.03	107	269
Snowpack-top five layers	-1.83	-2.33	0.24	1.13	57	270

**Table 6.** Correlation coefficient between different snowpack parameters

	Slope of line (k/Hz; H-Pol)/ slope of line (k/Hz; V-Pol)	Weighted average snowpack density (g/cm <sup>3</sup> )	Weighted average snowpack temperature (K)	Snowpack depth (cm)	Weighted average snowpack wetness (vol. %)
Slope of line (k/Hz; H-Pol) Slope of line (k/Hz; V-Pol)	1.00/1.00	-0.99/-0.99	-0.92/-0.92	0.92/0.92	-0.84/-0.85
Weighted average snowpack density (g/cm <sup>3</sup> )	-0.99/-0.99	1.00	0.86	-0.87	0.77
Weighted average snowpack temperature (K)	-0.92/-0.92	0.86	1.00	-0.99	0.98
Snowpack depth (cm)	0.92/0.92	-0.87	-0.99	1.00	-0.98
Weighted average snowpack wetness (% vol.)	-0.84/-0.85	0.77	0.98	-0.98	1.00

was dry/moist, the frequencies 18.7 and 37 GHz were used for snow depth estimation. However, for Dhundhi 37 GHz channels were used as the snowpack was observed thin in that region and use of low frequencies 6.9 and 18.7 GHz can introduce errors in the result because of their higher penetration.

The measured  $T_B$  values corresponding to the snowpack before and after removal of different snow layers were used to develop the snow depth algorithms. The difference in  $T_B$  values at 18.7 and 37 GHz (H) for Patseo and at 37 GHz (H) for Dhundhi was considered in the equations. Figure 12 *a* shows the variation in difference in  $T_B$  at 18.7 and 37 GHz frequency with varying snow depth values, whereas Figure 12 *b* shows the variation in  $T_B$  with snow depth at 37 GHz frequency. From Tables 2 and 3, it can be observed that with snow depth variation the snow properties also changed at both Dhundhi and Patseo. However, this change in snow properties, i.e. density, hardness and moisture content in different snow layers was observed to be high in Dhundhi in comparison to Patseo (Tables 2 and 3). Due to high variation in snow layer properties at Dhundhi, it was observed that with the removal of each snow layer, the  $T_B$  variation was significant and the same can be observed from Figure 12 *b* as well. However, at Patseo the  $T_B$  variation was not very

significant until the removal of five snow layers from the top of snowpack. However, high variation in  $T_B$  was observed by removing the snow layers near the ground, i.e. when the snowpack was comparatively thin. The empirical relations between  $T_B$  and snow depth were obtained from these experiments and correlation coefficient between these two factors was observed to be 0.9 for Patseo and 0.8 for Dhundhi.

These empirical relations were further applied on satellite data to estimate the snow depth from the other areas in the Greater Himalaya range. The estimated snow depth values for certain locations in the Greater Himalaya range using the above-mentioned empirical relation were compared with measured values, as shown in Figure 13. Both the values were found to be comparable (absolute error varied between 7 and 39 cm). This proves that although the equation for snow depth estimation was formulated from the results of field experiment conducted at Patseo, it can be applied to estimate snow depth from larger areas. This equation can also be used for estimation of snow depth from Karakoram and Pir-Panjal range but the error in estimated snow depth values will be higher.

The developed snow depth equation from field experiment conducted at Dhundhi was also used to estimate the snow depth using satellite data. From the developed

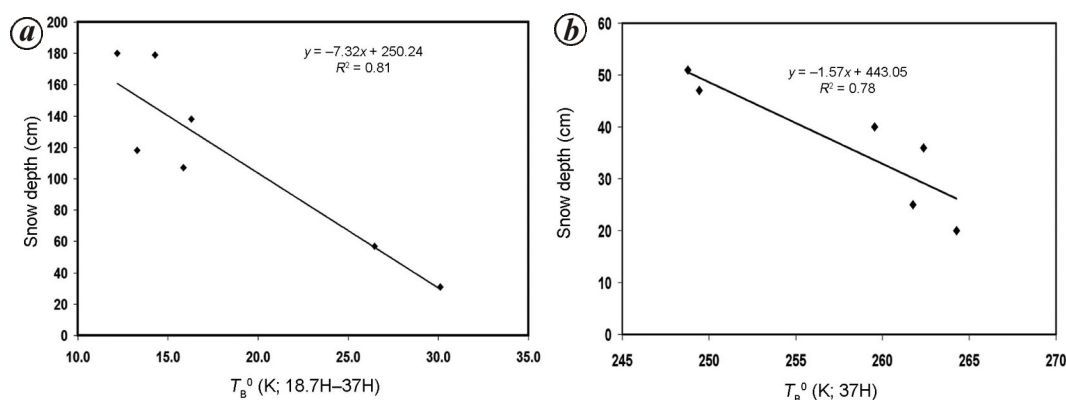


Figure 12. Snow depth algorithm developed from field experiments at (a) Patseo and (b) Dhundhi.

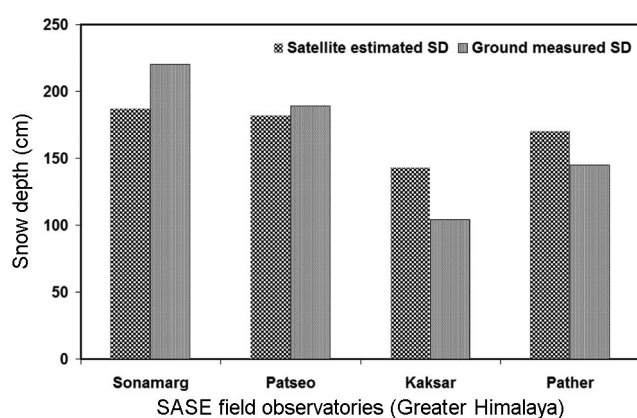


Figure 13. Comparison of satellite data-estimated snow depth (SD) with ground-measured values at some locations in the Greater Himalaya.

equation the satellite-estimated snow depth at Dhundhi on 13 March 2009 was 74 cm; however, ground measured value was 60 cm. Further, this equation was used to estimate the snow depth from other locations of the Pir-Panjal range, but was not found suitable. High spatial variability of snow cover and high ambient temperature in the Pir-Panjal range along with the presence of trees and vegetation may be some of the factors affecting the result of the equation. In the Pir-Panjal range, the fraction of tree and vegetation is high in comparison to the Greater Himalaya and this factor significantly affects the microwave radiation captured at the satellite level.

## Conclusion

Experimental results reported in this article show the use of passive microwave radiometer for estimation of snow depth for the Himalayan terrain. The qualitative and quantitative snowpack parameters were measured manually and using snow fork. The  $T_B$  values were estimated at 6.9, 18.7 and 37 GHz frequencies, at different polarizations and their variation with varying snowpack param-

eters was also analysed. The late winter wet/very wet snowpack at Dhundhi showed different characteristics at microwave frequencies in comparison to the peak winter dry/moist snowpack at Patseo. The  $T_B$  of snow was observed to be much higher at Dhundhi (Pir-Panjal) in comparison to Patseo (Greater Himalaya). Due to highly varying snow layer properties, the variation of  $T_B$  with snow depth was much higher at Dhundhi in comparison to Patseo. Decrease in  $T_B$  was observed with increase in snow depth, except for few snow layers where due to the lower values of snow density, an increase in  $T_B$  was observed. High values of  $T_B$  at 37 GHz in comparison to 6.9 and 18.7 GHz can be used as an indicator for the presence of wet/very wet snow. MEMLS was used to simulate the microwave emissions from the snowpack at varying frequencies. The offset applied MEMLS output  $T_B$  values were found to be closer to the experimental  $T_B$  values. The advantage of using this model is that the snow characteristics are studied at individual layers and this has provided an understanding of the penetration and attenuation of microwave radiations.

The radiometer data with respect to the snowpack before and after the removal of snow layers one by one from the top were further used to develop the snow depth algorithm. The algorithm was developed based on the field experiments conducted at Patseo and Dhundhi, which are the representative of the Greater Himalaya and Pir-Panjal range respectively. The snow depth algorithm was further applied on satellite data to estimate snow depth from larger areas. The satellite-estimated snow depth values were found to be closer to ground measured values at various locations in the Himalaya. The results were better for the Greater Himalaya in comparison to the Pir-Panjal range, as the vegetation and high spatial variability of snow cover in the latter affect the performance of the algorithm. Overall this passive microwave radiometer-based methodology can provide useful information of snow depth from the large area, which is otherwise difficult to collect. Conducting such experiments is important to improve understanding of the complex influence

of different snow characteristics (grain size, density, moisture, snow temperature) on the microwave emission and on snow retrievals from microwave measurements. In the near future with more field experiments conducted at good spatially varying locations, the snow depth can be estimated with greater accuracy using a combination of field and satellite data.

1. Sekar, K. C., Invasive alien plants of Indian Himalayan region – diversity and implication. *Am. J. Plant Sci.*, 2012, **3**, 177–184.
2. Sharma, S. S. and Ganju, A., Complexities of avalanche forecasting in Western Himalaya – an overview. *Cold Reg. Sci. Technol.*, 2002, **31**, 95–102.
3. Shekhar, M. S., Chand, H., Kumar, S., Srinivasan, K. and Ganju, A., Climate-change studies in the western Himalaya. *Ann. Glaciol.*, 2010, **51**, 105–112.
4. Kulkarni, A. V., Singh, S. K., Mathur, P. and Mishra, V. D., Algorithm to monitor snow cover using AWiFS data of RESOURCESAT-1 for the Himalayan region. *Int. J. Remote Sensing*, 2006, **27**(12), 2449–2457.
5. Mishra, V. D., Gusain, H. S. and Arora, M. K., Algorithm to derive narrow band to broad band albedo for snow using AWiFS and MODIS imagery of Western Himalaya – validation. *Int. J. Remote Sensing Appl.*, 2012, **2**(1), 1–9.
6. Das, I. and Sarwade, R. N., Snow depth estimation over north-western Himalaya using AMSR-E. *Int. J. Remote Sensing*, 2008, **29**, 4237–4248.
7. Colbeck, S. C., An overview of seasonal snow metamorphism. *Rev. Geophys. Space Phys.*, 1982, **20**, 45–46.
8. Stiles, W. H. and Ulaby, F. T., Dielectric properties of snow. The University of Kansas, Center for Research, Inc., RSL Technical Report 527-1, 1981.
9. Grody, N. C., Relationship between snow parameters and microwave satellite measurements: theory compared with advanced Microwave sounding unit observations from 23 to 150 GHz. *J. Geophys. Res.*, 2008, **113**, 1–17; doi: 10.1029/2007JD009685.
10. Wiesmann, A. and Mätzler, C., Microwave emission model of layered snowpacks. *Remote Sensing Environ.*, 1999, **70**, 307–316.
11. Negi, H. S., Mishra, V. D., Singh, K. K. and Mathur, P., Application of ground penetrating radar for snow, ice and glacier studies. In Proceedings of the International Symposium on Snow Monitoring and Avalanches, Snow and Avalanche Study Establishment (SASE), Manali, 12–16 April 2004.
12. Singh, K. K., Kulkarni, A. V. and Mishra, V. D., Estimation of glacier depth and moraine cover study using ground penetrating radar (GPR) in the Himalayan region. *J. Indian Soc. Remote Sensing*, 2010, **38**, 1–9.
13. Chang, A. T. C., Kelly, R. E. J., Foster, J. L. and Hall, D. K., Global SWE monitoring using AMSR-E data. In Geoscience and Remote Sensing Symposium, IGARSS'03, Proceedings, 2003, vol. 1, pp. 680–682; doi: 10.1109/IGARSS.2003.1293880.
14. Foster, J. L., Chang, A. T. C. and Hall, D. K., Comparison of snow mass estimates from a prototype passive microwave snow algorithm, a revised algorithm and a snow depth climatology. *Remote Sensing Environ.*, 1997, **62**, 132–142.
15. Kelly, R. E., Chang, A., Tsang, L. and Foster, J. L., A prototype AMSR-E global snow area and snow depth algorithm. *IEEE Trans. Geosci. Remote Sensing*, 2003, **41**, 230–242.
16. Wiesmann, A. and Mätzler, C., Microwave emission model of layered snowpacks. *Remote Sensing Environ.*, 1999, **70**, 307–316.
17. Pulliainen, J., Grandell, J. and Hallikainen, M., HUT snow emission model and its applicability to snow water equivalent retrieval. *IEEE Trans. Geosci. Remote Sensing*, 1999, **37**, 1378–1390.
18. Singh, K. K., Mishra, V. D. and Negi, H. S., Evaluation of snow parameters using passive microwave remote sensing. *Def. Sci. J.*, 2007, **57**, 271–278.
19. Singh, K. K., Mishra, V. D. and Garg, R. K., Microwave response of seasonal snow cover measured by using a ground-based radiometer at 6.93 and 18.7 GHz frequencies and at dual polarization. *J. Indian Soc. Remote Sensing*, 2007, **35**, 243–251.
20. Denoth, A., An electronic device for long term snow wetness recording. *Ann. Glaciol.*, 1994, **19**, 104–106.
21. User/Technical Manual of Snow Fork, the Portable Snow Properties Measuring Instrument, Ins. toimisto Toikka Oy, Hannuntie 18,02360 Espoo, Finland, 2010.
22. Gusain, H. S., Chand, D., Thakur, N. K., Singh, A. and Ganju, A., Snow avalanche climatology of Indian Western Himalaya. In Proceedings of the International Symposium on Snow and Avalanches, SASE, Manali, 6–10 April 2009.
23. Microwave remote sensing: Land and ocean surface applications, Meteorology Education and Training, COMET Program, University Corporation for Atmospheric Research (UCAR); <http://www.meted.ucar.edu>
24. Mätzler, C., Relation between grain size and correlation length of snow. *J. Glaciol.*, 2002, **48**, 461–466.

ACKNOWLEDGEMENTS. We thank Shri Ashwagosha Ganju (Director, SASE, Chandigarh) for motivation and support; Dr C. Mätzler (University of Bern, Switzerland) for providing the MEMLS model. Dr V. D. Mishra, Shri H. S. Gusain and Shri Piyush Joshi (SASE, Chandigarh) for technical discussions and those at SASE who helped in the collection of the ground data. We also thank the National Snow and Ice Data Center, University of Colorado, Boulder for the AMSR-E data.

Received 24 February 2014; revised accepted 27 November 2014